Comprehensive pharmacogenomic profiling of malignant pleural mesothelioma identifies a subgroup sensitive to FGFR inhibition.

Josine M. Quispel-Janssen[2,5*] , Jitendra Badhai[2*], , Laurel Schunselaar[2*],Stacey Price[1] ,Jonathan Brammeld[1], Francesco Iorio[3], Krishna Kolluri[4], Matthew Garnett[1], Anton Berns[2], , Paul Baas[2,6], Ultan McDermott[1,6] Jacques Neefjes[2,6], Constantine Alifrangis[1,5,6]

[1] Wellcome Trust Sanger Institute, Hinxton, UK
[2] Netherlands Cancer Institute, Amsterdam, Netherlands
[3] European Bioinformatics Institute, Hinxton, UK
[4] UCL Dept of Respiratory Medicine, London, UK
[5] Corresponding authors
[6] Senior authors

*** Equal contribution**

Running title: Profiling of MPM identifies FGFR-inhibitor sensitive subgroup

Keywords: mesothelioma, FGFR, BAP1, biomarker

Translational relevance

Malignant pleural mesothelioma (MPM) has limited treatment options and a dismal prognosis. To date targeted therapies have proved ineffective and no druggable genetic alterations have been identified. Selecting compounds for further clinical evaluation in this small and heterogeneous patient group is challenging. By combining high-throughput drug screens, comprehensive molecular characterisation and functional assays in multiple mesothelioma models, we were able to identify a FGFR inhibitor-sensitive subgroup with BAP1 loss as a potential predictive biomarker. Loss of BAP1 is found in up to 64% of MPM tumours. These data suggest that a significant group of patients with mesothelioma may benefit from FGFR inhibition.

ABSTRACT

Purpose: Despite intense research, treatment options for patients with mesothelioma are limited and offer only modest survival advantage. We screened a large panel of compounds in multiple mesothelioma models, and correlated sensitivity with a range of molecular features to detect biomarkers of drug response.

Experimental design: We utilised a high-throughput chemical inhibitor screen in a panel of 889 cancer cell lines, including both immortalised and primary early passage mesothelioma lines, alongside comprehensive molecular characterisation using Illumina whole exome sequencing, copy number analysis and Affymetrix array whole transcriptome profiling. Subsequent validation was done using functional assays such as siRNA silencing and mesothelioma mouse xenograft models.

Results: A subgroup of immortalized and primary MPM lines appeared highly sensitive to FGFR inhibition. None of these lines harboured genomic alterations of FGFR family members, but rather BAP1 protein loss was associated with enhanced sensitivity to FGFR inhibition. This was confirmed in a MPM mouse xenograft model and by BAP1 knock-down and overexpression in cell line models. Gene expression analyses revealed an association between BAP1 loss and increased expression of the receptors FGFR1/3 and ligands FGF9/18. BAP1 loss was associated with activation of MAPK signalling. These associations were confirmed in a cohort of MPM patient samples.

Conclusion: A subgroup of mesotheliomas cell lines harbour sensitivity to FGFR inhibition. BAP1 protein loss enriches for this subgroup, and could serve as a potential biomarker to select patients for FGFR inhibitor treatment. These data identify a clinically relevant MPM subgroup for consideration of FGFR therapeutics in future clinical studies.

INTRODUCTION

Malignant Pleural Mesothelioma (MPM) is a tumour arising from the pleural cavity and is strongly associated with occupational exposure to asbestos. Although strict regulation is in place in more than 50 countries, in parts of the world where there is still widespread usage of asbestos, most notably in South America, Russia and states of the former Soviet Republic, China and South-East Asia, the incidence of this disease is rising. [2]. MPM is highly refractory to conventional anti-cancer therapies and the prognosis is poor; most patients die within a year of diagnosis. Surgery with curative intent is only possible in a highly selected group of patients and needs to be combined with chemotherapy. The only approved treatment, a combination of the cytotoxic agents cisplatin and pemetrexed, yields at best modest improvements in survival [3] [4]. Despite many clinical studies utilising novel biological therapies, there are as yet no effective targeted therapies for this cancer [5] [6].

A recent comprehensive genomic analysis of 216 MPM samples found *BAP1, NF2, TP53, SETD2* and *CDKN2A* to be recurrently mutated or structurally rearranged [7]. The landscape is thus one of mutated tumour suppressor genes and alterations in pathways as diverse as Hippo, mTOR and TP53, as well as histone methylation. Such loss-of-function oncogenic events are typically considered "undruggable", but downstream programs of genes, activated as a consequence of such mutations, may themselves be tractable therapeutic targets. This is illustrated by NF2-deficient tumours with activated Focal Adhesion Kinase (FAK). Defactinib, a FAK inhibitor demonstrated efficacy in NF2-deficient tumours *in vitro* [8] but a subsequent clinical trial in mesothelioma was halted due to lack of efficacy. Other drugs tested to date which have failed to improve the outcome in MPM include EGFR inhibitors [9], Bcr-Abl inhibitors [10], thalidomide [11], bortezomib [12] and vorinostat [13]. In many of these studies a subgroup of patients appeared to derive some benefit. However, in MPM, it has been difficult to elucidate reproducible biomarkers that identify these sensitive subgroups. Some research groups have demonstrated co-activation of multiple RTK pathways in MPM tumours which may provide a rationale for combination therapies with kinase inhibitors [14].

We aimed to utilise high-throughput chemical screening platforms alongside molecular characterisation of immortalised and early passage cell line models of MPM to uncover critical signalling pathways that may be amenable to therapeutic interrogation.

Materials and methods

Cell lines and tissue culture

Cells are grown and maintained in either RPMI or DMEM F/12 supplemented with 10% FBS and 1% penicillin/streptomycin. Cell lines were maintained at 37°C at 5% CO2. All cell lines have been verified by genotyping using Short Tandem Repeat (STR) profiling and Sequenom profiling of a panel of 92 Single nucleotide polymorphisms.

Cell viability Assays

Cells are trypsinised and counted before seeding at the optimal density for the well-size (either 96 or 384 well plates were used) and duration of the assay. Seeding density was optimised by titration of the cells such that upon visual inspection of the control wells at the end of the assay, a confluency of 70-90% was observed allowing cells to grow in a linear phase. Adherent cell lines were seeded 24 hrs before drug addition. The high-throughput chemical inhibitor screen was carried out using 384-well plates and viability was measured 72 hours after drug addition with a 5-point serial 4-fold concentration range of 265 compounds. All other viability assays were carried out using 96-well plates and a 9-point two-fold dilution of the drugs. Drugs were all dissolved in DMSO and DMSO only was used as a control condition. At the end of the experiment, cells were fixed with 4% paraformaldehyde. Following two washes with dH_2O, 100µl of Syto60 nucleic acid stain (Invitrogen) was added to a final concentration of 1µM (a 1/5000 stock dilution) and plates were fixed for 1hr at room temperature. Quantification of fluorescent signal was achieved using a Paradigm (BD) plate reader using excitation/emission wavelengths of 630/695 nM. Data was analysed by adjusting for background signals and normalising each well to the DMSO treated control.

High-throughput Screening Compounds

Compounds were acquired from academic collaborators or commercial vendors. Each compound, its therapeutically relevant target substrate and pathway and the minimum and maximum screening concentrations are listed in Supplemental Table S1. Compounds were stored as 10 μM aliquots at −80°C and were subjected to a maximum of 5 freeze-thaw cycles. Each of the agents was screened at a 5-point serial 4-fold dilution to provide a 256-fold range from the lowest to highest concentration. The concentrations selected for each compound were based on *in vitro* data to cover the range of concentrations known to inhibit relevant kinase activity and cell viability.

Apoptosis assay

Cells were seeded in a flat bottom 384 wells plate at optimal cell density. After 24 hours PD173074 and AZD 4547 in a concentration range between 0,007813 and 1uM were added using a Tecan HP D300 Digital Dispenser. Five replicate wells were assayed for each condition. Phenylarsine oxide (20 uM) was used as positive control condition. To assess apoptosis, 5uM of IncuCyte caspase-3/7 green apoptosis assay reagent was added to the cells. Confluence and apoptosis levels were quantified by IncuCyte Zoom live-cell imaging systems from Essen bioscience. Relative apoptosis was calculated by dividing the confluence of fluorescent apoptotic cells by total confluence and normalized to the positive control condition.

Western Blots

Cell monolayers were lysed on ice in NP40 Cell Lysis Buffer (Invitrogen) containing fresh Protease and Phosphatase inhibitors (Roche). Lysates were centrifuged at 13000 rpm for 10 minutes and the supernatant used for analyses. Protein concentration was calculated from a standard curve of BSA using the BCA assay (calbiotech) according to manufacturer's instructions. Equal protein concentrations were loaded on pre-cast 4-12% Bis–Tris SDS-PAGE Gels (Invitrogen), run at 200V for 1 hr. Proteins were transferred onto a methanol activated PVDF membrane at 100V for 1 hr or overnight at 30V. Membranes were blocked in 5% milk for 1 hour before the addition of primary antibody at a

concentration recommended. After overnight incubation with the primary antibody at 4°C, the membrane was washed three times in 0.1% TBS-T followed by incubation with the secondary antibody according to supplier's description at 1/2500 dilution). Immunoblots were imaged using Pierce Supersignal Plus chemiluminescent kit on a gel imager (Syngene). Antibodies against BAP1, pERK, ERK, pFGFR (total) and pFGFR1 (all from Cell Signalling Technologies) and the polyclonal p-FGFR3 antibody sc-33041 (Santa Cruz) were used. Beta Tubulin was used as a loading control for western blots. Phospho RTK arrays (RD systems) and Caspase-Glo 3/7 Assay were used according to the manufacturer's instructions.

Establishment of early passage primary mesothelioma tumor cell cultures

All patients whose materials were used, provided written informed consent for the use and storage of pleural fluid, tumor biopsies and germ line DNA. Diagnosis was made on tumor biopsies according to local IHC protocols and confirmed by the Dutch Mesothelioma Panel, a national expert panel of certified pathologists that evaluate all suspected mesothelioma patient samples. Early passage primary mesothelioma cultures were generated from tumor cells isolated from pleural fluid of patients at the Netherlands Cancer Institute. The pleural fluid was centrifuged at 1500 rpm for 5 minutes at room temperature. Erythrocyte lysis buffer was used to remove erythrocytes if many were present. Cells were resuspended in Dulbecco's Modified Eagle Medium (DMEM, Gibco) supplemented with peniciline/streptomycin and 8% fetal calf serum. The cells were seeded in T75 flasks at a density of $1x10^6$ cells/ml and incubated at 37°C at a humidified 5% CO_2 atmosphere. Medium was refreshed depending on cell growth, usually twice a week. At seeding and during the first 2 passages, cytospins were made and stained with HE and reviewed by our pathologist to determine the percentage of tumor cells. If the tumor percentage was over 70%, usually reached after 1 passage, living cell cultures were transported to the Wellcome Trust Sanger Institute within 6 hours for drug screening and genetic analysis. Cells were cultured for a maximum period of 4 weeks.

RNA interference and transfection

Lipofectamine RNAiMAX (Thermofisher) was used according to product guidelines for transfection with siRNA against FGFR3 (Thermo Fisher Silencer Select s5167 and s5169) or BAP1 (s15822) utilising the protocol 'forward transfection of mammalian cell lines'. KIF11 siRNA (s7902) was used as a transfection (positive) control. Viability or protein expression were assayed as described above, at specified time points. H226 cell expressing a BAP1 stable construct, and BAP1 C91A mutant lines were a kind gift from K Kolluri (UCL, London).

Gene expression analyses

Microarray data was generated on the Human Genome U219 96-Array Plate using the Gene Titan MC instrument (Affymetrix). The robust multi-array analysis (RMA) algorithm (Irizarry et al., 2003) was used to establish intensity values for each of 18562 loci (BrainArray v.10,)We discarded transcripts with low sample variance and consolidated duplicated genes by averaging their expression values across duplicates. The resulting data were subsequently normalised (μ=0, σ=1) sample-wise and gene-median centred. Raw data was deposited in ArrayExpress (accession: E-MTAB-3610).

The RMA processed dataset is available at

(www.cancerrxgene.org/gdsc1000/GDSC1000_WebResources/Home.html).

The expression level signal of each gene was normalised using a non-parametric kernel estimation of its cumulative density function as described in [38]. Additionally the normalised expression values were further tissue-centred using as grouping factors the cell line tissue labels of [39].

MPM Mouse Xenograft Models

All animal experiments were conducted according to institutional guidelines under protocol approved by the animal ethics committee of the Netherlands Cancer Institute. To establish xenografts, three million human mesothelioma cells (H2731 and MSTO211H) were implanted subcutaneously into the right dorsal flank of 6-7 weeks old female nude SCID mice. Mice were randomized into vehicle and drugs treatment groups and treatment was initiated once the tumour volumes reached approximately 200 mm^3. Tumour size was measured with

callipers twice a week and tumour volume was determined as a × b^2 × 0.5, where a and b were the large and small diameters, respectively.

RESULTS

High-throughput chemical inhibitor screens in immortalised cell lines

A panel of 889 cancer cell lines was screened with 265 compounds that included targeted and cytotoxic compounds (for detail see **http://www.cancerrxgene.org/**). It was observed that 3 of 19 MPM lines (H2795, H2591 and MSTO-211H) had IC50 values among the top 5% of cell lines showing highest sensitivity to the compound PD-173074, an FGFR1 and FGFR3 kinase inhibitor (**Figure 1A**) [15]. These three cell lines, together with two additional MPM lines (NCI-H28 – resistant, MPP-89 – partially sensitive) and a FGFR-dependent lung cancer cell line harbouring amplification of FGFR1 (NCI-H1581), were re-screened with PD-173074 and were as sensitive to PD-173074 as the FGFR1-dependent lung cancer line NCI-1581 (**Figure 1B**). Furthermore this sensitivity was also seen with two more selective FGFR inhibitors, NVP-BGJ398 and AZD4547 (**Figure S1).** Sensitivity to PD-173074 in the MPM cell lines was confirmed by clonogenic survival assays (**Figure 1C**). Although some sensitive lines died by apoptosis as is shown by activated caspase activity with both PD-173074 and the multi FGFR targeted inhibitor AZD4547 (**Figure 1D,1E**), not all sensitive lines showed a dose incremental increase in this marker. These data confirm previous findings [25] that a subset of MPM cell lines require FGF pathway activation for growth and survival, and that targeting this pathway could be a critical step in the control of these tumours.

Drug sensitivity in early passage MPM cultures

To test whether these observations could be reproduced in an independent cohort of primary mesothelioma cell lines, a panel of 11 pleural fluid-derived early passage cultures from patients with MPM tumours were obtained and screened for viability using a panel of 48 small molecule inhibitors including PD-173074. Most of the early passage cultures were resistant to virtually all agents (**Figure S2**). However, one MPM early passage culture (NKI04) did demonstrate marked sensitivity to PD-173074. The sensitivity of

NKI04 to FGFR inhibition was confirmed in a longer duration clonogenic survival assay, and the effect on cell viability was comparable to that seen in the FGFR1-amplified NCI-H1581 lung cancer cell line (**Figure 2A-2C**).

Molecular characterisation of FGF pathway signalling in cell lines and patient samples

In order to understand the basis for the observed sensitivity to FGFR inhibition, we analysed whole exome sequence and copy number array data for 21 MPM lines (http://cancer.sanger.ac.uk/cell_lines). There was no evidence of activating mutations or whole gene amplifications in any FGFR family member. RNA sequencing has been undertaken and shows no evidence of a fusion transcript involving any member of the FGFR family in any of the MPM cell lines (personal communication M Garnett). We then analysed the corresponding gene expression data and focussed on differential expression of FGFR and FGF family members in PD-173074 sensitive and resistant MPM cell lines. Normalised expression of each of the FGF and FGFR family genes was correlated with sensitivity to PD-173074 to explore whether the variation in any single family member, either ligand or receptor, was associated with response to FGFR-inhibition. We found a statistically significant correlation between elevated FGF9 mRNA expression and response to PD-173074 ($p=0.0148$) and AZD4547 treatment (P0.0098) (**Figure 3A).** FGF9 is a secreted, high affinity ligand for the FGFR3 receptor, with low affinity for the FGFR1 and FGFR2 receptors [16]. To determine whether a subset of MPM exhibits elevated expression of the FGF9 ligand in patients, we analysed gene expression from a panel of 53 assorted MPM and matched normal lung clinical samples (**Figure 3B**) [17]. Overall, we observed significantly higher FGF9 transcript levels in MPM tumours compared to pleura and lung normal tissue ($p<0.0001$). Therefore, similar to our observation in the MPM cell lines, a subset of patient samples also demonstrates high levels of FGF9 expression.

Modulation of FGF/FGFR function in MPM lines

A possible premise for the observed sensitivity of MPM lines that express high levels of FGF9 would be activation of the FGFR3 receptor kinase in an autocrine loop and subsequent engagement of pro-survival downstream signalling pathways. Indeed, a comparison of phosphorylation status of 42 receptor tyrosine kinases between a small sample of MPM cell lines demonstrated increased phosphorylation of FGFR3 in the sensitive line H2795 but not in resistant lines Met-5A and NCI-H28 (**Figure 3C**).

To further confirm a critical role for FGFR3, this transcript was silenced by siRNA in a panel of MPM cell lines and the direct effect on cell viability was measured. Transient siRNA mediated silencing of the FGFR3 transcript reduced cell viability in all 3 FGFR-inhibitor sensitive cell lines, but not in the FGFR-inhibitor resistant lines. This indicates a dependency on FGFR3 mediated signalling of the FGFR-inhibitor sensitive lines (**Figure 3D**). As would be expected, inhibition of FGFR3 by the specific inhibitors AZD4547 and BJG398 decreased pERK levels (**figure 3E**) and this was also seen following siRNA mediated silencing of FGFR3 in H2795 and MSTO-211H (**Figure 3F**). The addition of FGF9 ligand to MPM cells lacking baseline FGFR3 activation was able to induce phosphorylation of FGFR3 and a change in the growth kinetics of this cell line in a dose dependent fashion (**Figure S5**).

Role of BAP1 in modulating FGF pathway signalling

Although we failed to identify genomic alterations in any member of the FGFR family that might explain the sensitivity to FGFR inhibition, we reasoned that this dependency might also be the consequence of other gene aberrations up- or downstream of FGFR3 signalling. We evaluated the gene expression and mutation database for other statistical associations explaining sensitivity to the FGFR-inhibitor AZD4547 in the panel of MPM cell lines. We focussed on driver mutations or copy number alterations in 3 of the most frequently mutated genes in MPM, namely *BAP1, NF2* and *CDKN2A* [7]. We detected a weak but non-significant association between AZD4547 sensitivity and *BAP1* mutations in the sensitive cell lines (**Figure 4A**). Given that loss of BAP1 protein expression might also occur through non-mutational mechanisms as previously described [37], we additionally characterised BAP1 protein status in these lines by Western blot

analysis (**Figure S3 and S4**). When sensitivity to the AZD4547 was correlated with BAP1 protein expression (low/absent vs expressed), there was a significant correlation between loss of BAP1 expression and sensitivity (p=0.0208) (**Figure 4B**).

Functional consequences of BAP1 modulation on FGFR signalling.

Since silencing FGFR3 reduced cell viability in a subset of MPM lines, we next investigated whether this dependency on FGFR signalling was regulated by BAP1. BAP1 is a nuclear deubiquitinating enzyme with many unelucidated functions that might include modulation of the FGFR pathway. Silencing of BAP1 expression resulted in increased phosphorylation of FGFR3 (**Figure 4C)**. Conversely, restoring BAP1 expression in the BAP1 null MPM line (**Figure 4D**) H226 resulted in a decrease in pFGFR and a modest increase in resistance to the FGFR inhibitor, AZD4547 (**Figure 4E**).

We observed increased expression at the protein level in the *BAP1* mutant cell lines of other RTK receptor genes and their appropriate ligands also known to be important in cell survival signalling in MPM such as PDGFRB, IGF1-R and MET [18] using phospho- RTK arrays (**Figure S4A and S4B**). The H226 null MPM cell line was transfected with a wild type BAP1 construct and a functionally inactive C91A mutant BAP1 construct. Gene expression analysis on these two lines was performed and Signalling Pathway Impact Analysis (SPIA) of the data (**Supplementary Table**) demonstrated that among the most significantly activated pathways in BAP1 inactive cells is the "Bladder Cancer" pathway including FGFR3 (arrow, **Figure S6A**) illustrated in **Figure S6B** [19]. In summary, the gene expression analysis demonstrates that BAP1 loss-of-function is associated with a transcriptional response upregulating not only FGFR signalling but also other RTK's such as PDGFRB, CMET and IGF1R, that may be important mediators of cell growth and survival. However, only FGFR inhibitors showed a significant viability effect as single agents. We analysed gene expression data from a study of 51 mesothelioma tumour samples to see if a similar effect on the FGFR pathway was seen in vivo (40 *BAP1* wild-type and 11 mutant) (GEO GSE29354) [20]. Amongst members of the FGFR signalling family, *BAP1* mutant tumours did indeed demonstrate increased expression of FGF18,

FGFR2 and FGFR3 relative to *BAP1* wildtype tumours (**Supplementary Table**). To explore this association further in human tumours we analysed the available TCGA data and looked for the incidence of genetic and mRNA alterations of these genes in MPM tumours by *BAP1* status (**Figure 4F**). This showed the majority of dysregulation (10 of 14) events in FGF9, FGF18 and FGFR3 occured in the context of BAP1 gene or mRNA dysregulation.

FGFR inhibition in MPM xenograft model

To assess the *in vivo* efficacy of targeting FGFR in MPM, we established a xenograft model using the FGFR-inhibitor sensitive MPM lines H2795 and MSTO-211H. Mice were treated with AZD4547, a selective inhibitor of FGFR1/2/3, which is currently being evaluated in clinical trials.. We observed that treatment with AZD4547 resulted in significant growth inhibition in the H2795- and MSTO-211H-derived tumours (**Figure 5A**). Furthermore, AZD45457 treated tumours showed a reduction in pERK signalling by immunohistochemistry compared to vehicle control treated tumours (**Figure 5B**) indicating target engagement by the drug in this model. Caspase activation was also seen in drug treated tumours suggesting apoptosis (**Figure S7**).

Combination therapeutic screen.

As the single agent efficacy of FGFR inhibition was only seen in a subset of MPM cell lines, and since persistent pAKT pathway activation was seen in cell lines not responsive to FGFR inhibition, we hypothesised that a combination screen utilising a PI3 kinase inhibitor may reveal useful synergies. We undertook an anchor-based combination screen in 15 MPM cell lines using 95 small molecule inhibitors (see supplemental table for details) selected to target many critical pathways in cancer, both as single agents and in combination with a fixed dose of the PI3 Kinase inhibitor AZD6482. . The resulting difference in Area Under the Curve (AUC) between single agent small molecule inhibitor and the combination with AZD6482, was used to calculate synergy. The most recurrent synergistic interactions were seen with IGF1R inhibitor BMS-536924 and FGFR inhibitor PD-173074 (**Figure S8A)** with synergy observed in 7 and 6 of 15 lines

409 respectively. **Figure S8B** shows a validation dose-response curve of the FGFRi
410 resistant NCI H28 cell lines showing minimal effect of BMS 536824 or AZD6482
411 alone, but reduced viability and pAKT reduction with the combination. This
412 cytotoxicity is not seen in the mesothelial control cell line Met5a suggesting the
413 synergy is not generic but cell line specific.
414
415
416
417
418
419
420
421
422

DISCUSSION

Since MPM is a rare and heterogeneous tumour, it is notoriously difficult to identify and characterize responding subgroups in clinical trials. Our work illustrates the application and possibilities of comprehensive pharmacogenomic profiling approaches in intractable cancers such as MPM. The finding of FGFR-inhibitor sensitivity in a subgroup of immortalised MPM cell lines represents a potentially novel therapeutic approach for this tumour type. As immortalised cell lines may undergo genetic drift, we also confirmed our findings in primary mesothelioma early passage lines.

Dysregulation of the FGFR pathway has been described in many cancer types [21, 22]. FGF9 signalling through FGFR3 has been shown to have a role in the development and progression of tumour cells in mouse models for NSCLC and prostate cancer [23]. In MPM cell lines models, we observed that high levels of the ligand FGF9 were strongly correlated with sensitivity to the FGFR-inhibitors PD-173074 and AZD4547. We hypothesise that the effects of FGF9 are mediated through FGFR3 signalling, as illustrated by modulation of downstream ERK phosphorylation upon chemical inhibition with small molecule inhibitors of FGFR3 and knockdown of FGFR3. FGFR3 is conversely not phosphorylated in cell lines insensitive to FGFRi, and this phosphorylation can be induced by the addition of synthetic FGF9 ligand. Interestingly, there was variability in FGF9 mRNA expression levels among the MPM cell lines, similar to what is observed in tumours in previously published studies. Recently, other groups demonstrated efficacy of FGFR inhibition in pre-clinical models of MPM mediated by other FGF-pathway members such as FGFR1 [24] [25] [26]. We confirm the efficacy of a clinically utilised FGFR inhibitors including AZD4547 in vivo in MPM xenograft models. Furthermore since undertaking these studies early phase clinical work with pharmacokinetic data have been published [42,43] on AZD4547 and BGJ398. These have confirmed that the doses used in the in vitro work (100nM to 1uM) here are achievable in plasma in vivo and are able to modulate the target, with pharmacodynamic end points of target engagement with FRS2 downregulation and changes in serum phosphate levels seen.

FGF receptors and ligands are being targeted in clinical trials by both selective and non-selective FGFR TKI's and monoclonal antibodies [27] and

AZD4547 has shown modest clinical activity in tumours with FGFR pathway aberrant activation [40]. In MPM dovitinib, a multi-targeting kinase inhibitor with activity against FGFR, has been trialled and has failed in small cohort of patients with MPM [41]. Since the data across tumour types demonstrate only a small group of patients responds to FGFR inhibition, it is crucial to find biomarkers that predict response to FGFR inhibition. Guagnano et al. integrated genomic and transcriptomic data of about 500 tumour cell lines with drug sensitivity data to find predictive biomarkers for response to FGFR inhibitor NVP-BGJ398. A genetic alteration in one of the four FGF receptors was found in 7% of cell lines but only about half of the cell lines with such an alteration was found to be sensitive [28].

We did not find any mutation, amplification or fusion transcripts of the FGFR family in the inhibitor-sensitive MPM cell lines. The genes that were most recurrently altered in our MPM cell lines include *CDKN2A, BAP1* and *NF2.* The frequency at which these genes were mutated is broadly similar to those previously described in clinical MPM samples [6] [7].

We show that loss of BAP1 expression was associated with sensitivity to FGFR inhibition. This finding was further validated with modulation of pFGFR signalling and dose response kinetics to FGFR inhibition following siRNA mediated knockdown and BAP1 overexpression in MPM cell lines. Caveats with this association were also observed: NCI-H28 was one of the most resistant cell lines to FGFR inhibition but carried a *BAP1* homozygous deletion, suggesting that BAP1 loss may enrich for FGFR-inhibitor sensitive cell lines but that some heterogeneity of drug response may still be observed. BAP1 (BRCA associated protein 1) is a nuclear deubiquinating enzyme that controls gene expression by interaction with numerous transcription factors and other complexes, including those of the double strand DNA break repair machinery [29]. BAP1 thus influences cell cycle progression [30] and double strand DNA break repair [31]. We show here that its loss may also affect gene expression of FGF pathway members, thereby enhancing signalling through this pathway.

The *BAP1* gene is inactivated by somatic mutation in 23-64% of patients with MPM and between 1-47% in other tumour types [20] [32] [33] [34].

Furthermore, BAP1 protein levels are undetectable in about 25% of MPM with normal *BAP1* gene status, likely by epigenetic modification [20]. BAP1 loss was observed to enrich for FGFR-inhibitor sensitive MPM lines, and expression of C91 hydrolase inactive mutant versus wild type BAP1 protein in the H226 cell line induced activation of FGFR3 signalling. We hypothesize that inactivation of BAP1 in MPM, possibly through its function as a ubiquitin hydrolase, induces changes in gene expression of both FGF family ligands and receptors to stimulate cell growth and survival.

We performed a combination drug screen to assess the impact of novel combinations of targeted therapies on MPM cell lines. On the 15 MPM cell lines screened we found that FGFR and IGF1R inhibitors were the most recurrently synergistic with the PI3-kinase inhibitor AZD6482. This is the first time to our knowledge that both a single agent and combination therapeutic screen have been performed which point to the primacy of the FGFR signalling pathway in MPM. Interestingly one of the most resistant cell lines to FGFR inhibition was amenable to treatment with AZD6482 plus IGF1R inhibition with evidence of ablation of pAKT with the combination of drugs but not with either alone, implying true synergy. Previous studies have identified that multiple RTK's are active in MPM [14], and this has provided some rationale to consider combination therapies to overcome innate resistance to targeted therapies. It is also interesting to speculate as to whether IGF1R plus Pi3K inhibition would be of use in acquired resistance to FGFR inhibitors.

CONCLUSION

High-throughput drug screening revealed a subset of both immortalized and primary mesothelioma cell lines to be highly sensitive to FGFR-inhibition.

This sensitivity was mediated through FGFR3, and was associated with loss of BAP1 protein expression. The high incidence of BAP1 protein loss in MPM tumours implies potential benefit from FGFR inhibition for a substantial subset of this patient group. In addition our anchor based screens revealed synergistic combinations that helped to overcome innate resistance to FGFR inhibition. (4409 words).

REFERENCES

1. van Meerbeeck, J.P., et al., *Malignant pleural mesothelioma: the standard of care and challenges for future management.* Crit Rev Oncol Hematol, 2011. **78**(2): p. 92-111.
2. Frank, A.L. and T.K. Joshi, *The global spread of asbestos.* Ann Glob Health, 2014. **80**(4): p. 257-62.
3. Baas P, Fennel DA et al *Malignant pleural mesothelioma: ESMO Clinical Practice Guidelines for diagnosis, treatment and follow-up.* Ann Oncol, 2015.
4. Vogelzang, N.J., et al., *Phase III study of pemetrexed in combination with cisplatin versus cisplatin alone in patients with malignant pleural mesothelioma.* J Clin Oncol, 2003. **21**(14): p. 2636-44.
5. Pinton, G., et al., *Therapies currently in Phase II trials for malignant pleural mesothelioma.* Expert Opin Investig Drugs, 2013. **22**(10): p. 1255-63.
6. Ladanyi, M., et al., *New strategies in pleural mesothelioma: BAP1 and NF2 as novel targets for therapeutic development and risk assessment.* Clin Cancer Res, 2012. **18**(17): p. 4485-90.
7. Bueno, R., et al., *Comprehensive genomic analysis of malignant pleural mesothelioma identifies recurrent mutations, gene fusions and splicing alterations.* Nat Genet, 2016. **48**(4): p. 407-16.
8. Shapiro, I.M., et al., *Merlin deficiency predicts FAK inhibitor sensitivity: a synthetic lethal relationship.* Sci Transl Med, 2014. **6**(237): p. 237ra68.
9. Govindan, R., et al., *Gefitinib in patients with malignant mesothelioma: a phase II study by the Cancer and Leukemia Group B.* Clin Cancer Res, 2005. **11**(6): p. 2300-4.
10. Mathy, A., et al., *Limited efficacy of imatinib mesylate in malignant mesothelioma: a phase II trial.* Lung Cancer, 2005. **50**(1): p. 83-6.
11. Baas, P., et al., *Thalidomide in patients with malignant pleural mesothelioma.* Lung Cancer, 2005. **48**(2): p. 291-6.
12. Fennell, D.A., et al., *Phase II clinical trial of first or second-line treatment with bortezomib in patients with malignant pleural mesothelioma.* J Thorac Oncol, 2012. **7**(9): p. 1466-70.

13. Krug, L.M., et al., *Vorinostat in patients with advanced malignant pleural mesothelioma who have progressed on previous chemotherapy (VANTAGE-014): a phase 3, double-blind, randomised, placebo-controlled trial.* Lancet Oncol, 2015. **16**(4): p. 447-56.
14. Menges, C.W., et al., *A Phosphotyrosine Proteomic Screen Identifies Multiple Tyrosine Kinase Signaling Pathways Aberrantly Activated in Malignant Mesothelioma.* Genes Cancer, 2010. **1**(5): p. 493-505.
15. Davis, M.I., et al., *Comprehensive analysis of kinase inhibitor selectivity.* Nat Biotechnol, 2011. **29**(11): p. 1046-51.
16. Zhang, X., et al., *Receptor specificity of the fibroblast growth factor family. The complete mammalian FGF family.* J Biol Chem, 2006. **281**(23): p. 15694-700.
17. Gordon, G.J., et al., *Identification of novel candidate oncogenes and tumor suppressors in malignant pleural mesothelioma using large-scale transcriptional profiling.* Am J Pathol, 2005. **166**(6): p. 1827-40.
18. Brevet, M., et al., *Coactivation of receptor tyrosine kinases in malignant mesothelioma as a rationale for combination targeted therapy.* J Thorac Oncol, 2011. **6**(5): p. 864-74.
19. Tarca, A.L., et al., *A novel signaling pathway impact analysis.* Bioinformatics, 2009. **25**(1): p. 75-82.
20. Bott, M., et al., *The nuclear deubiquitinase BAP1 is commonly inactivated by somatic mutations and 3p21.1 losses in malignant pleural mesothelioma.* Nat Genet, 2011. **43**(7): p. 668-72.
21. Dienstmann, R., et al., *Genomic aberrations in the FGFR pathway: opportunities for targeted therapies in solid tumors.* Ann Oncol, 2014. **25**(3): p. 552-63.
22. Helsten, T., et al., *The FGFR Landscape in Cancer: Analysis of 4,853 Tumors by Next-Generation Sequencing.* Clin Cancer Res, 2016. **22**(1): p. 259-67.
23. Suzuki, T., et al., *Multiple roles of extracellular fibroblast growth factors in lung cancer cells.* Int J Oncol, 2015. **46**(1): p. 423-9.
24. Schelch, K., et al., *Fibroblast growth factor receptor inhibition is active against mesothelioma and synergizes with radio- and chemotherapy.* Am J Respir Crit Care Med, 2014. **190**(7): p. 763-72.

25. Marek, L.A., et al., *Nonamplified FGFR1 is a growth driver in malignant pleural mesothelioma.* Mol Cancer Res, 2014. **12**(10): p. 1460-9.
26. Plones, T., et al., *Absence of amplification of the FGFR1-gene in human malignant mesothelioma of the pleura: a pilot study.* BMC Res Notes, 2014. **7**: p. 549.
27. Touat, M., et al., *Targeting FGFR Signaling in Cancer.* Clin Cancer Res, 2015. **21**(12): p. 2684-94.
28. Guagnano, V., et al., *FGFR genetic alterations predict for sensitivity to NVP-BGJ398, a selective pan-FGFR inhibitor.* Cancer Discov, 2012. **2**(12): p. 1118-33.
29. Yu, H., et al., *The ubiquitin carboxyl hydrolase BAP1 forms a ternary complex with YY1 and HCF-1 and is a critical regulator of gene expression.* Mol Cell Biol, 2010. **30**(21): p. 5071-85.
30. Eletr, Z.M. and K.D. Wilkinson, *An emerging model for BAP1's role in regulating cell cycle progression.* Cell Biochem Biophys, 2011. **60**(1-2): p. 3-11.
31. Yu, H., et al., *Tumor suppressor and deubiquitinase BAP1 promotes DNA double-strand break repair.* Proc Natl Acad Sci U S A, 2014. **111**(1): p. 285-90.
32. Yoshikawa, Y., et al., *Frequent inactivation of the BAP1 gene in epithelioid-type malignant mesothelioma.* Cancer Sci, 2012. **103**(5): p. 868-74.
33. Nasu, M., et al., *High Incidence of Somatic BAP1 alterations in sporadic malignant mesothelioma.* J Thorac Oncol, 2015. **10**(4): p. 565-76.
34. Murali, R., T. Wiesner, and R.A. Scolyer, *Tumours associated with BAP1 mutations.* Pathology, 2013. **45**(2): p. 116-26.
35. Lu, C., et al., *The genomic landscape of childhood and adolescent melanoma.* J Invest Dermatol, 2015. **135**(3): p. 816-23.
36. Carbone, M., et al., *Combined Genetic and Genealogic Studies Uncover a Large BAP1 Cancer Syndrome Kindred Tracing Back Nine Generations to a Common Ancestor from the 1700s.* PLoS Genet, 2015. **11**(12): p. e1005633.
37. Shah, A.A., T.D. Bourne, and R. Murali, *BAP1 protein loss by immunohistochemistry: a potentially useful tool for prognostic prediction in patients with uveal melanoma.* Pathology, 2013. **45**(7): p. 651-6.

38. Hanzelmann S, Castelo R, Guinney J. GSVA: Gene set variation analysis for microarray and RNA-seq data. BMC Bioinformatics 2013. **14**(7) p1471-2105.

39. Iorio F et al. A Landscape of Pharmacogenomic interactions in cancer. Cell 2016 **166** (3) p740-754.

40. Paik PK, Shen R, Berger MF, Ferry D, Soria JC, Mathewson A, Rooney C, Smith NR, Cullberg M, Kilgour E, Landers D, Frewer P, Brooks N, André F.*A Phase Ib Open-Label Multicenter Study of AZD4547 in Patients with Advanced Squamous Cell Lung Cancers.* Clin Cancer Res. 2017 Sep 15;23(18):5366-5373. doi: 10.1158/1078-0432.CCR-17-0645. Epub 2017 Jun 14. PMID:28615371

41. Laurie SA, Hao D, Leighl NB, Goffin J, Khomani A, Gupta A, Addison CL, Bane A, Seely J, Filion ML, Pond GR, Levine MN. *A phase II trial of dovitinib in previously-treated advanced pleural mesothelioma: The Ontario Clinical Oncology Group.* Lung Cancer. 2017 Feb;104:65-69. doi: 10.1016/j.lungcan.2016.12.004. Epub 2016 Dec 15. PubMed PMID: 28213002.

42. Nogova L, Sequist LV, Perez Garcia JM, Andre F, Delord JP, Hidalgo M, Schellens JH, Cassier PA, Camidge DR, Schuler M, Vaishampayan U, Burris H, Tian GG, Campone M, Wainberg ZA, Lim WT, LoRusso P, Shapiro GI, Parker K, Chen X, Choudhury S, Ringeisen F, Graus-Porta D, Porter D, Isaacs R, Buettner R, Wolf J. *Evaluation of BGJ398, a Fibroblast Growth Factor Receptor 1-3 Kinase Inhibitor, in Patients With Advanced Solid Tumors Harboring Genetic Alterations in Fibroblast Growth Factor Receptors: Results of a Global Phase I, Dose-Escalation and Dose-Expansion Study*. J Clin Oncol. 2017 Jan 10;35(2):157-165. Epub 2016 Nov 21.

43. Gavine PR, Mooney L, Kilgour E, Thomas AP, Al-Kadhimi K, Beck S, Rooney C, Coleman T, Baker D, Mellor MJ, Brooks AN, Klinowska T. *AZD4547: an orally bioavailable, potent, and selective inhibitor of the fibroblast growth factor receptor tyrosine kinase family.* Cancer Res. 2012 Apr 15;72(8):2045-56. doi: 10.1158/0008-5472.CAN-11-3034. Epub 2012 Feb 27. PubMed PMID: 22369928.

FIGURE LEGENDS

Figure 1.
Sensitivity to FGFR-inhibition in established mesothelioma cell lines.
A, Sensitivity to FGFR-inhibitor PD173074 expressed as logIC50 value (inhibiting concentration that kills 50% of the cells) of each different cell line. The enlargement shows the 5% most sensitive cell lines with amongst them mesothelioma cell lines depicted in red.

B, Dose-response curves depicting the cell viability (mean ±SD) of different cell lines (y-axis) as a function of the dose of FGFR-inhibitor PD-173074. NCI-H28, MPP-89, H2810 and H2795 are mesothelioma cell lines, while NCI-H1581 is a FGFR-dependent lung cancer cell line.

C, Fourteen-day clonogenic survival assay of selected mesothelioma cell lines (NCI-H28, MSTO-211H, H2810, H2795), treated with FGFR-inhibitor PD-173074 at concentrations of 500nM and 1uM.

D, FGFR-inhibitor AZD4547 kills mesothelioma cell lines via induction of apoptosis as is demonstrated by an increase in caspase 3/7 activity after 48 hours of treatment with different doses of AZD4547 in a panel of MPM cell lines,

E, FGFR-inhibitor PD173074 kills mesothelioma cell lines via induction of apoptosis as is demonstrated by an increase in caspase 3/7 activity after 48 hours of treatment with different doses of PD-173074 a panel of MPM cell lines,

Figure 2.
Sensitivity to FGFR-inhibitors in primary mesothelioma lines and xenograft mouse models.
A, Cell viability (mean ±SD) of primary mesothelioma line NKI04 after treatment with a fixed does of 48 different small molecule inhibitors. This cell line is most sensitive to FGFR-inhibition.

B, Fourteen-day clonogenic survival assay of primary mesothelioma line NKI04 compared to immortalized mesothelioma line NCI-H28 treated with FGFR-inhibitor PD-173074 at concentrations of 500nM and 1uM.

C, Cell viability (mean ±SD) of primary mesothelioma line NKI04 compared to immortalized mesothelioma line NCI-H28 and FGFR-dependent lung cancer cell line NCI-H1581 (y-axis), as a function of the concentration of FGFR-inhibitor PD-173074. NCI-H28, MPP-89, H2810 and H2795 are mesothelioma cell lines

Figure 3.
FGFR-inhibitor sensitivity is mediated by FGF axis signaling through FGF9 and FGFR3.
A, Scatterplot depicting sensitivity to FGFR-inhibitor PD-173074 as a function of expression of FGF9 . mRNA. Y axis depicting log mRNA expression of FGF9 and x – axis showing centile of Ic50 to PD173074 of individual MPM cell line in cell line screen. High FGF9 gene expression is significantly correlated to high sensitivity to FGFR-inhibition. Right hand scatterplot showing s FGF9 expression correlates with sensitivity to AZD4547 .

B, Expression of FGF9 in a set of MPM tumours, compared to normal lung and pleura, derived from GE0 dataset GSE2549. The mean expression in MPM tumours is significantly higher than that of normal lung and pleura.

C, Phospho-RTK Array reveals phosphorylated-FGFR3 in FGFR-inhibitor sensitive cell line H2795 that is absent in 2 resistant lines (NCI-H28 and Met5a).

D, Cell viability of MPM cell lines after silencing of the FGFR3 transcript demonstrates reduced viability of FGFR-inhibitor sensitive cell lines H2795, H2810 and H2731 compared to FGFR-inhibitor resistant lines Met5A, NCI-H2052, H2810 and MPP89. Viability at 4Days post transfection is compared to Kif11 positive control siRNa and Scrambled negative control.

E. Modulation of pERK signaling in H2795 cell line following 6 hours of exposure to DMSO (C) or 500nM AZD4547 or DMSO and 100nM BGJ398.

F. siRNA mediated knockdown of pFGFR3 in H2795 and MSTO211H, showing effect on pFGFR3 and pERK versus scrambled control.

Figure 4.
Loss of BAP1 protein expression is correlated to FGFR-inhibitor sensitivity.
A, Sensitivity to FGFR-inhibitor AZD4547 -expressed as logIC50 value- of cell lines, grouped according to *BAP1* mutation status. The mean logIC50 value is not significantly different between the two groups.

B, Sensitivity to FGFR-inhibitor AZD4547 according to BAP1 protein expression. Red are cell lines with low or absent BAP1 protein. Blue lines have normal BAP1 protein expression. Sensitivity (left) is expressed as logIC50 value (y-axis). The difference between the two groups is statistically significant. Cell viability (right) of different mesothelioma lines (y-axis) after treatment with FGFR-inhibitor AZD4547 (x-axis). wt = wild type, mt = mutant, high = high protein expression, low = low protein expression, nil = no protein expression. Right hand panel showing dose-response curves of MPM cell lines treated with FGFR-inhibitor AZD4547. Cell lines in red are lines with low or absent BAP1 protein expression. Blue lines have normal BAP1 protein expression.

C SiRNA mediated depletion of BAP1 in H2052 at increasing siRNA doses of 5nM and 10nM versus mock transfected (M) control. Western blot comparing pFGFR3 and BAP1 expression at these conditions. Tubulin as loading control.

D. BAP1 overexpression in BAP1 null cell line H226. Western blot of BAP1 construct versus parental cell line baseline pFGFR levels with tubulin as loading control.

E, Cell viability after treatment with increasing doses of FGFR-inhibitor AZD4547 in parental cell line H226 BAP1 null (red) and in the same cell line with BAP1 construct (red).BAP1 overexpression increases cell viability after FGFR inhibition.

Figure 5.
Xenograft mouse model shows FGFR inhibition efficacy in vivo.

A, Xenograft mouse model using mesothelioma cell lines H2795 and MSTO211H. Mean tumour volume is depicted on the y-axis as a function of time (x-axis). Red lines indicate tumour growth in mice treated with FGFR-inhibitor AZD4547, while the black lines indicate growth in vehicle-treated mice.

B, Immunohistochemistry of AZD4547 vs vehicle control treated xenograft tumours. ppERK expression in representative tumours in drug treated vs vehicle control groups.

Figure 1

A

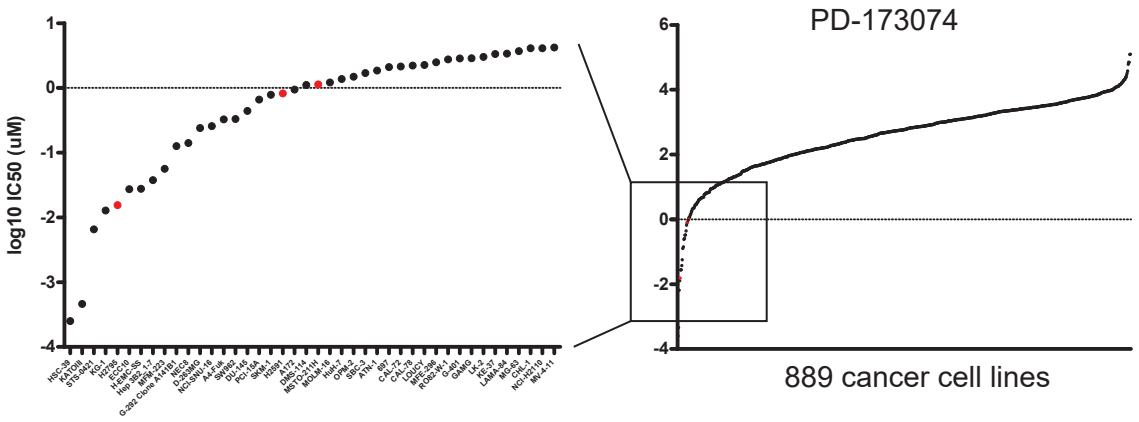

B

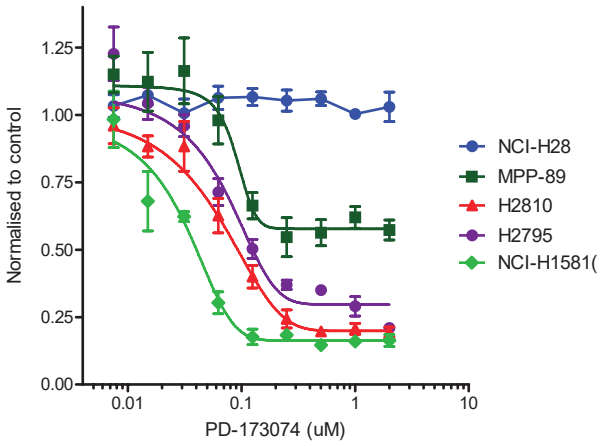

C

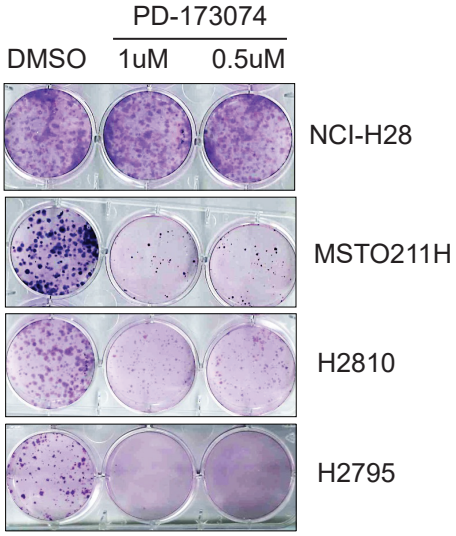

D

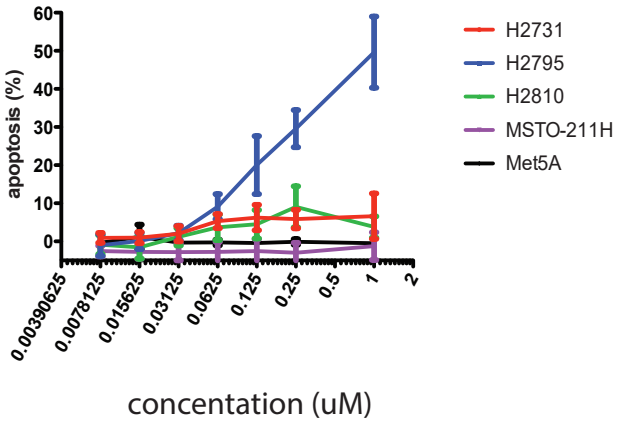

E

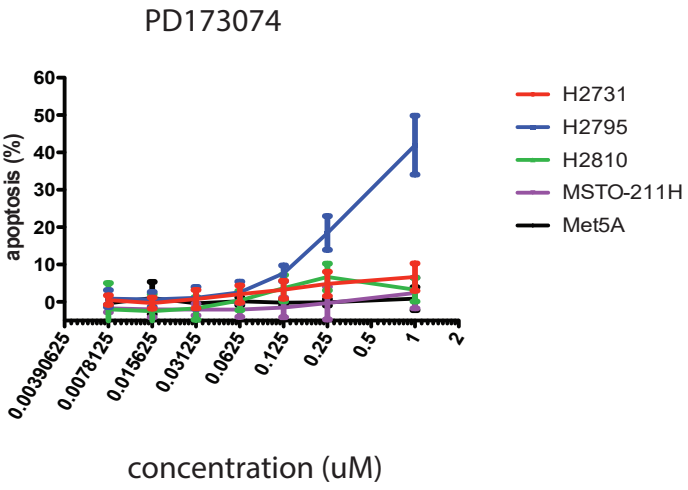

Figure 2

A

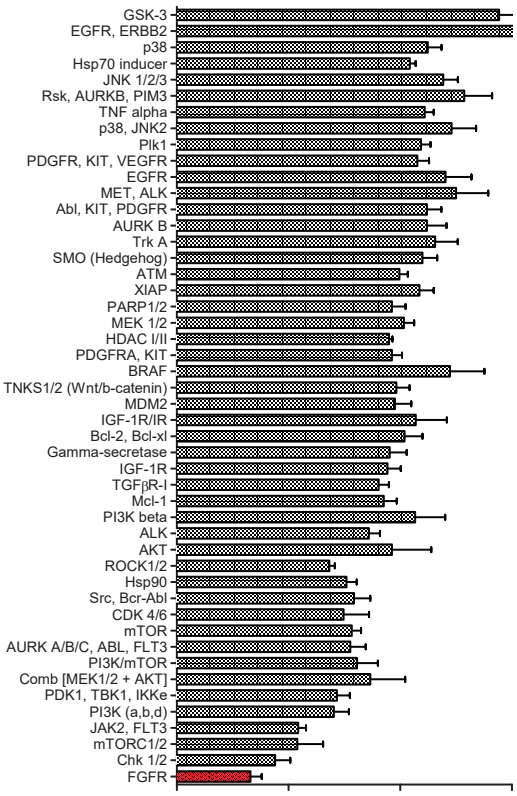
GSK-3
EGFR, ERBB2
p38
Hsp70 inducer
JNK 1/2/3
Rsk, AURKB, PIM3
TNF alpha
p38, JNK2
Plk1
PDGFR, KIT, VEGFR
EGFR
MET, ALK
Abl, KIT, PDGFR
AURK B
Trk A
SMO (Hedgehog)
ATM
XIAP
PARP1/2
MEK 1/2
HDAC I/II
PDGFRA, KIT
BRAF
TNKS1/2 (Wnt/b-catenin)
MDM2
IGF-1R/IR
Bcl-2, Bcl-xl
Gamma-secretase
IGF-1R
TGFβR-I
Mcl-1
PI3K beta
ALK
AKT
ROCK1/2
Hsp90
Src, Bcr-Abl
CDK 4/6
mTOR
AURK A/B/C, ABL, FLT3
PI3K/mTOR
Comb [MEK1/2 + AKT]
PDK1, TBK1, IKKe
PI3K (a,b,d)
JAK2, FLT3
mTORC1/2
Chk 1/2
FGFR

B

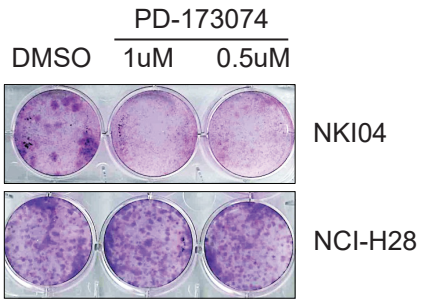
PD-173074
DMSO
1uM
0.5uM
NKI04
NCI-H28

C

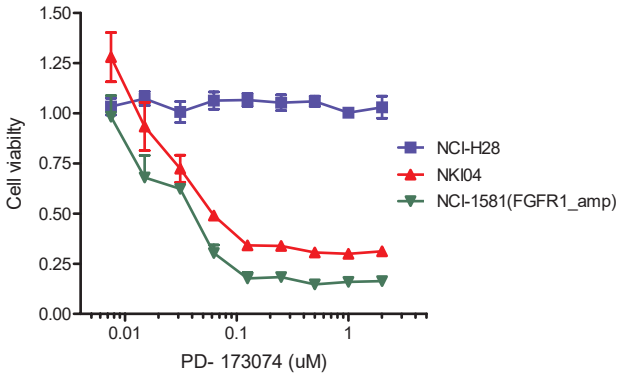
1.50
1.25
1.00
0.75
0.50
0.25
0.00
Cell viability
0.01
0.1
1
PD- 173074 (uM)
NCI-H28
NKI04
NCI-1581(FGFR1_amp)

Figure 3

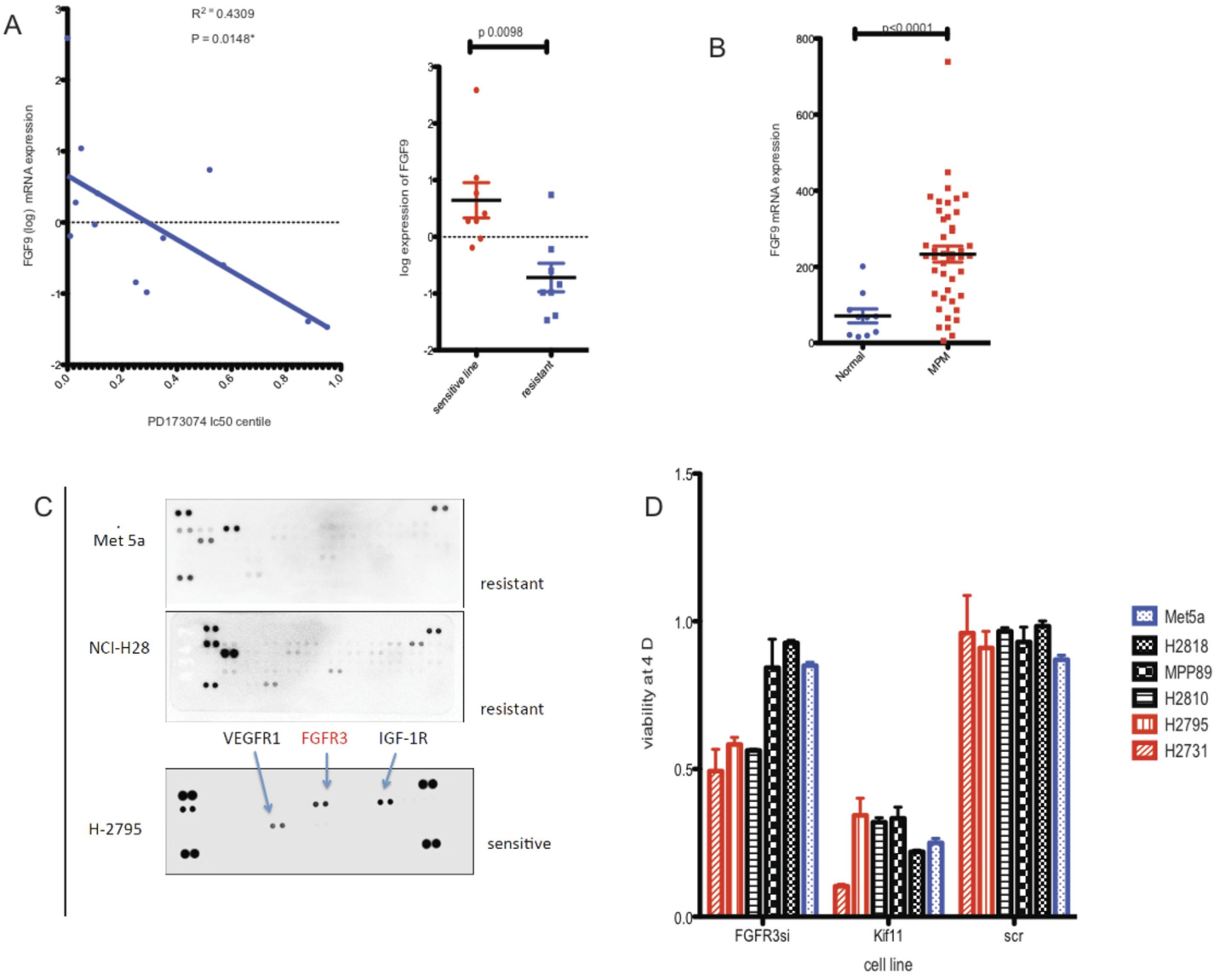
A
R² = 0.4309
P = 0.0148*
FGF9 (log) mRNA expression
PD173074 Ic50 centile
p 0.0098
log expression of FGF9
sensitive line
resistant
B
p<0.0001
FGF9 mRNA expression
Normal
MPM
C
Met 5a
resistant
NCI-H28
resistant
VEGFR1
FGFR3
IGF-1R
H-2795
sensitive
D
viability at 4 D
FGFR3si
Kif11
scr
cell line
Met5a
H2818
MPP89
H2810
H2795
H2731
E
H2795
C
AZD
C
BGJ
pAKT
pERK
B-Tubulin
F
H2795 MSTO
si scr si scr
pFGFR3
pERK
Actin

Figure 4

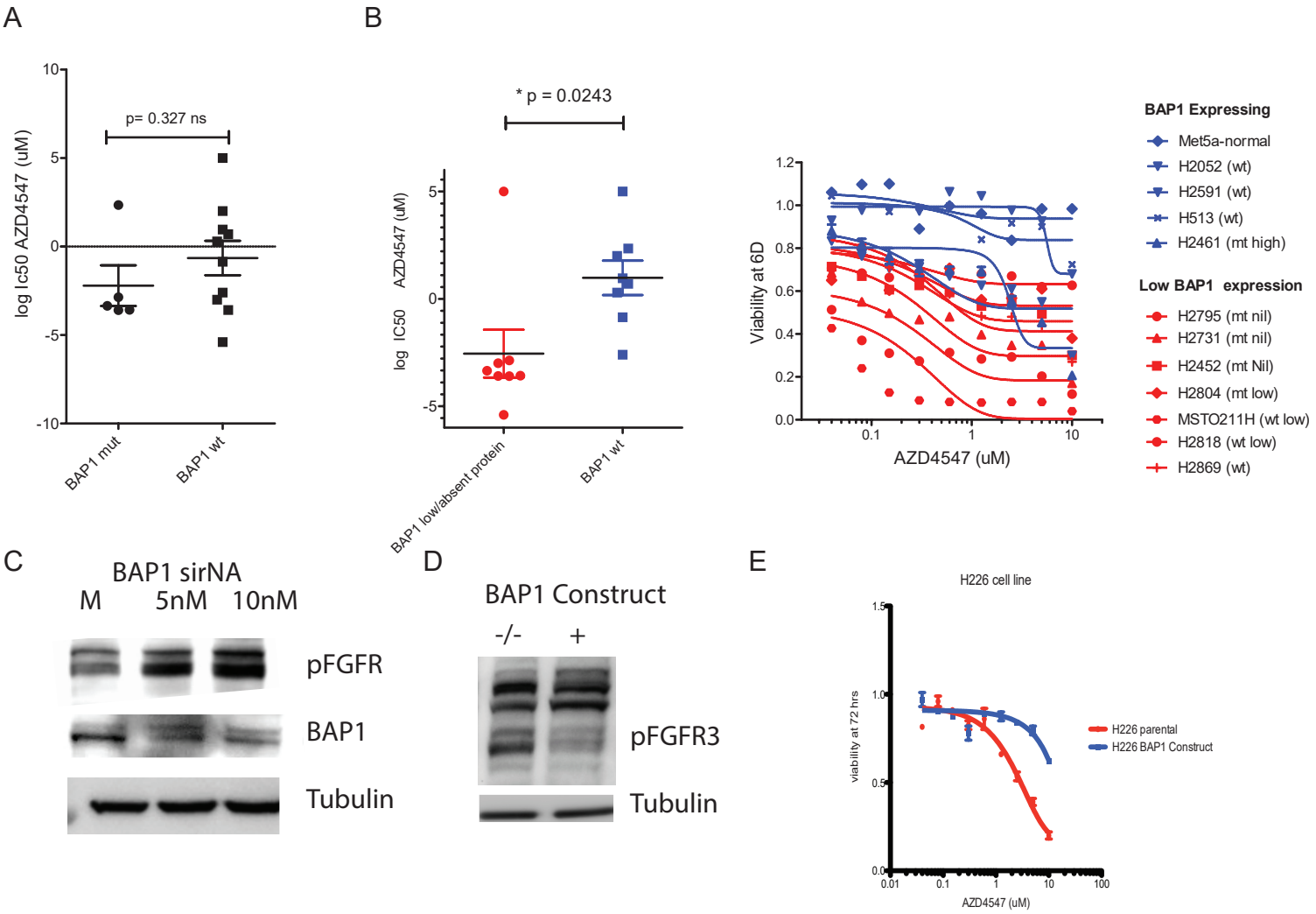
A
B
p= 0.327 ns
log Ic50 AZD4547 (uM)
BAP1 mut
BAP1 wt
* p = 0.0243
log IC50 AZD4547 (uM)
BAP1 low/absent protein
BAP1 wt
Viability at 6D
AZD4547 (uM)
BAP1 Expressing
Met5a-normal
H2052 (wt)
H2591 (wt)
H513 (wt)
H2461 (mt high)
Low BAP1 expression
H2795 (mt nil)
H2731 (mt nil)
H2452 (mt Nil)
H2804 (mt low)
MSTO211H (wt low)
H2818 (wt low)
H2869 (wt)
C
BAP1 sirNA
M
5nM
10nM
pFGFR
BAP1
Tubulin
D
BAP1 Construct
-/-
+
pFGFR3
Tubulin
E
H226 cell line
viability at 72 hrs
AZD4547 (uM)
H226 parental
H226 BAP1 Construct

F


BAP1 45%
FGFR3 3%
FGF9 6%
FGF18 7%
Genetic Alteration
Amplification
Deep Deletion
mRNA Upregulation
mRNA Downregulation
Truncating Mutation (putative drive
Missense Mutation (putative driver)

Figure 5

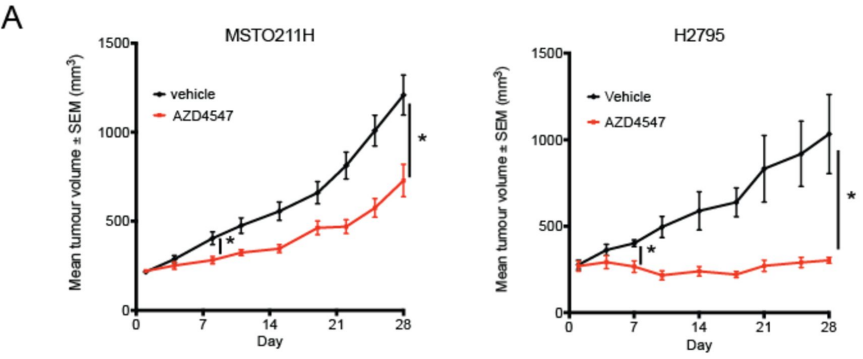
A
MSTO211H
H2795
vehicle
AZD4547
Vehicle
AZD4547
Mean tumour volume ± SEM (mm3)
Day
0
500
1000
1500
0
7
14
21
28
*

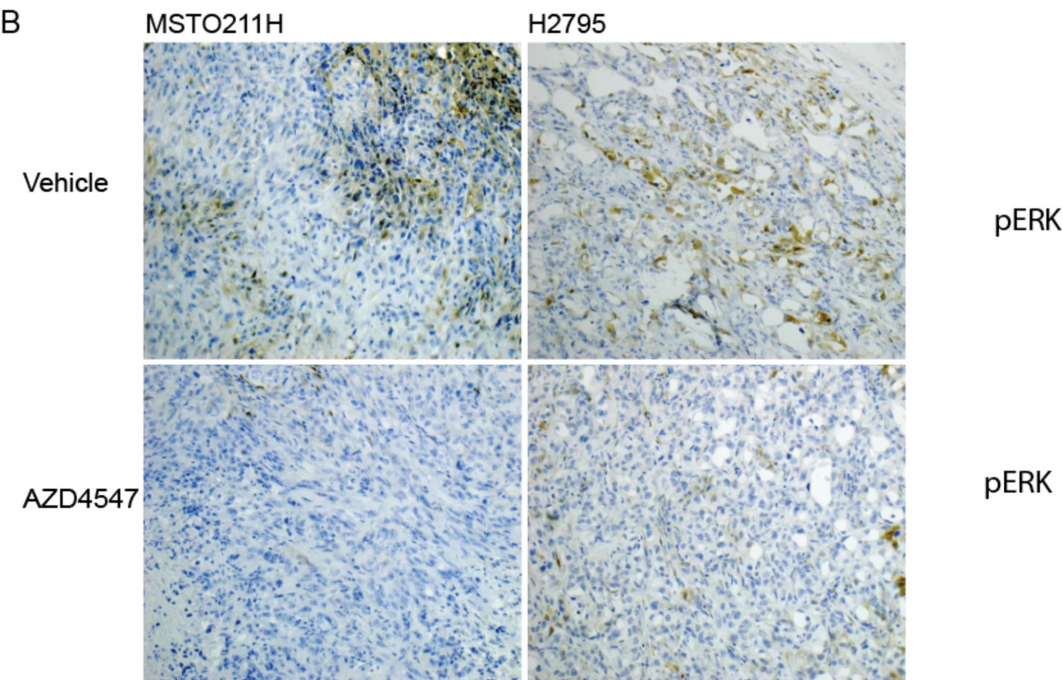
B
MSTO211H
H2795
Vehicle
AZD4547
pERK
pERK